Energy & Buildings 315 (2024) 114302

Contents lists available at ScienceDirect

Energy & Buildings

journal homepage: www.elsevier.com/locate/enbuild

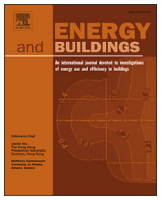

Analysis of a domestic air heat pump integrated with an air-geothermal heat exchanger in real operating conditions: The case study of a single-family building

Giovanna Cavazzini, Giacomo Zanetti, Alberto Benato *

Department of Industrial Engineering, University of Padova, Via Venezia 1, Padova, 35131, Italy

ARTICLE INFO

Keywords:
Air heat pumps
HVAC efficiency
Air-geothermal heat exchanger
Earth–air heat exchanger
Control strategy
Ventilation

ABSTRACT

The work presents an in-depth analysis of the real performance of an air heat pump unit installed in a single-family building and quantitatively determines the reduction in energy consumption achieved by the integration of an air-geothermal heat exchanger. The case study is a single-family building located in northern Italy. It is equipped with a heating, ventilation, and air conditioning (HVAC) system consisting of an air-geothermal heat exchanger coupled with a compact air source heat pump supported by an electric heater installed in a thermal storage and devoted to cover the peak demand. The main objectives of the work are to analyse the HVAC performance under real operating conditions compared to the design values and to highlight the existence of factors that affect this performance. The analysis was carried out by developing an accurate model of the heat pump system based on the real operating data acquired by the on-board monitoring system. The results confirmed the influence of the air-inlet conditions (temperature and humidity) and of the control strategy (more specifically, the ventilation flow rate) on the unit performance in both the heating and cooling modes. In particular, the analysis showed that minimising indoor ventilation in the case of low outdoor temperatures is of paramount relevance not only because it reduces the indoor heat demand, but also because it maintains the unit efficiency close to the design values. Furthermore, the installation of a geothermal heat exchanger guarantees a reduction in electricity consumption of approximately 30%.

1. Introduction

To achieve the goal of a climate-neutral society by 2050, the need to decarbonise the residential sector is of paramount importance. In fact, 85% of the EU buildings were built before 2000 and 75% of them have poor energy performance. In addition, around 40% of the energy consumed in the EU is used in buildings, more than a third of the EU's energy-related greenhouse gas emissions come from buildings and more or less 80% of the energy used in EU houses is for heating, cooling and domestic hot water production [1]. Therefore, renovating existing buildings could reduce the total energy consumption of the EU and reduce carbon dioxide emissions. Among the possible actions, one of the most important is to increase the share of power systems using renewable energy sources; one of the most valuable options to achieve this goal is electrification of residential heating and cooling demands. This is a change that can be achieved with a wide spread of heat pump technology, which combines the use of electricity with a high-efficiency energy conversion process.

A proof of the recognised role that this technology can play in the transition of building heating and cooling to a more sustainable sector is the volume of sales of heat pumps in Europe. In the last decade, European sales have increased significantly, but 2021 and 2022 were years with a huge growth rate: +34% and +38%, respectively. The latter means 3 million units sold in one year; a number that (i) avoids the combustion of approximately 4 billion cubic metres of natural gas, (ii) prevents the emissions of 8 million tonnes (Mt) of CO_2, and (iii) pushes the European connected heating heat pumps and hot water heat pumps up to 20 million, which corresponds to avoid 54 Mt of CO_2. A quota approximately equal to the equivalent annual emissions of a country like Greece [2].

Despite the promising growth in sales at the European level, heat pumps provide heating to approximately 16% of European residential

* Corresponding author.
E-mail address: alberto.benato@unipd.it (A. Benato).

https://doi.org/10.1016/j.enbuild.2024.114302
Received 3 July 2023; Received in revised form 30 April 2024; Accepted 15 May 2024
Available online 21 May 2024

and commercial buildings [3]. In fact, heat pumps are the preferred choice in new single-family buildings (more than 50% in France, Germany and Austria), but their penetration decreases in the new multi-family buildings (5% in France and 20% in Germany and Austria) and it is even lower in the case of renovation of old buildings, which represent in some countries a large share of the buildings in the residential sector (e.g., in Italy 86% of the buildings have been built before the 1990s and 57% before the 1960s [4]).

The reasons for this trend are several and not all are purely technical. In the vast majority of cases, the maintenance/installation of the carbon-based heating systems is preferred because these systems are perceived by the building owners/inhabitants as a well-known and, hence, "safer" choice from a techno-economical point of view. These subjective and often wrong opinions are encouraged by the differences between the manufacturers' declared performance and those in real operating conditions. The main reason for these differences is that the manufacturers data sheet refers to very specific conditions, which can significantly differ from real ones, where several parameters (climate area, temperature variability, control strategy, etc.) affect the in-operation performance of heat pump-based heating and cooling systems.

To provide more realistic information on the performance of heat pumps, several studies have been carried out. Among them, it is worth mentioning the study by Ruhnau et al. [5], proposing estimated time series of the heat pump coefficient of performance (COP) for different heat sources and sinks. These time series were obtained starting from the data provided by the manufacturers properly processed according to the quadratic regression method proposed by Fischer et al. and applying a constant correction factor of 0.85 [6]. The idea of considering a correction factor of 0.85 was first introduced by Gunther et al. [7] to better approximate the performance of the units under real operating conditions. Although the approach of Ruhnau et al. [5] is effective in reducing the overestimation of the heat pump performance, the choice of a constant correction factor did not significantly increase the precision of the analysis.

To address this knowledge gap, some authors performed laboratory tests [8], even combined with simulations [9], as well as different modelling strategies [10]. Wide trials in domestic buildings were also carried out in the UK [11] and Germany [12], highlighting the lack of satisfactory explanations for the wide variation in the efficiency of heat pump systems within the same group and compared to other country-based trials. These and more studies are also presented by Carrol et al. [13] in a recently published review on air heat pumps. The common framework in all these studies is the great influence that operating conditions can have on heat pump performance and the difficulty in identifying factors that cause performance not in line with expectations and also affect the operating costs of commercial solutions [14].

In this context, it is difficult to promote the penetration of innovative solutions that clearly favour an increase in performance, as is the case for geothermal heat pumps or earth-air heat exchangers.

The positive contribution of geothermal heat pumps was demonstrated more than ten years ago, for example, by Omer [15], highlighting the benefits of the almost constant subsurface temperature in the COP. More recently, even geothermal district heating systems [16] have been modelled and investigated under hypothetical operating conditions or experimentally analysed on the test platform [17]. To support the penetration of this innovation in the market, economical evaluations were also presented, such as that of Kulcar et al. [18], who analysed the profitability of investing in a geothermal heat pump.

Referring to the integration of Earth-Air heat exchangers to reduce the heating and cooling demands of buildings, only a few numerical and experimental investigations (see, e.g. [19–21]) were carried out. However, none of them has analysed from the experimental and numerical viewpoints the benefit of integrating this system with the heat pump technology (building an air-geothermal heat exchanger) and then comparing the datasheet performance with the real ones. Furthermore, none of the available literature was able to separate, under real operating conditions, the contribution of the air-geothermal heat exchanger to the reduction in energy consumption of all other factors that affect the performance of the heat pump system.

To this end, this work presents an in-depth investigation of the behaviour of an air-geothermal heat pump system installed in a single-family building. An accurate model has been developed and calibrated using the data acquired by the on-board monitoring system. Then, the model has been used to identify the main factors affecting the performance of the system in real operating conditions, and hence to quantitatively determine the reduction in energy consumption due to the integration of the air-geothermal heat exchanger in the heating/cooling system. The paper is organised as follows. Section 2 presents the case study and the commercial heating/cooling system, Section 3 describes the approach adopted to model the heat pump unit, based on monitored data, while Section 4 discusses the results of the analysis, identifying the real operating parameters that affect the performance of the heat pump and estimating the reduction in energy consumption that can be attributed to the air-geothermal heat exchanger. Finally, Section 5 provides concluding remarks.

2. Case study

The case study was a passive house located in Valtellina (climatic zone F - 3987 degree days - no limitations for both the heating period and the number of hours), with a net conditioned volume of 392 m^3 and a net area of 140 m^2. The structure was 10 cm thick Xlam [22], 24 cm of rock wool insulation, while the wooden roof was ventilated and insulated by 30 cm thick rock wool.

The air conditioning unit, whose simplified layout is depicted in Fig. 1, was an all-air type unit composed of three elements: a preheating/precooling air-geothermal heat exchanger (component 1), a heat pump unit (components 2-10) and an integrative post-heating thermal resistance (component 11).

The air-geothermal heat exchanger (component 1 in Fig. 1), whose design specification cannot be published for confidentiality reasons, has a pre-reception function: it preheats and pre-cools the air during the heating and cooling seasons, respectively. This layout guaranteed an almost constant temperature in the heating and cooling seasons independently of the outdoor air temperature, as clearly shown in Fig. 2. Fig. 2 shows the evolution in 2019 of the outdoor air temperature (t_{EXT}) and the pretreated air temperature (t_{GEO}) measured in the inlet and outlet section of the air-geothermal heat exchanger.

In the winter season even if the outdoor temperature fell below 0 °C (see t_{EXT} in Fig. 2), the air temperature supplied by the heat exchanger to the heat pump was never lower than 9 °C, while during the summer season the geothermal unit guaranteed a temperature not higher than 21.5 °C (see t_{GEO} in Fig. 2), despite the peaks at more than 30 °C of the outdoor air temperature.

The heat pump unit (components 2-10 in Fig. 1) was a Nilan Compact P model [23] and functioned as an HVAC system and a generator of domestic hot water (DHW), while thermal resistance (component 11 in Fig. 1) guaranteed the heat supply requirements during periods of high heat demand. The system is equipped with an on-board partial monitoring system, which allowed the measurement of some operating parameters. The performance of the heat pump declared by the manufacturer in both heating and cooling modes is given in Table 1. The unit is designed to operate in a standalone configuration, and therefore the air input can be outdoor air in the case of direct supply from the outdoor environment or air pretreated by the air-geothermal exchanger, as in the case study.

The main components of the unit depicted in Fig. 1 were:

- The passive heat recovery exchanger (component 3), exchanging energy between the exhaust air of the indoor environment sucked by the ventilation system and the inlet air. The heat exchanger

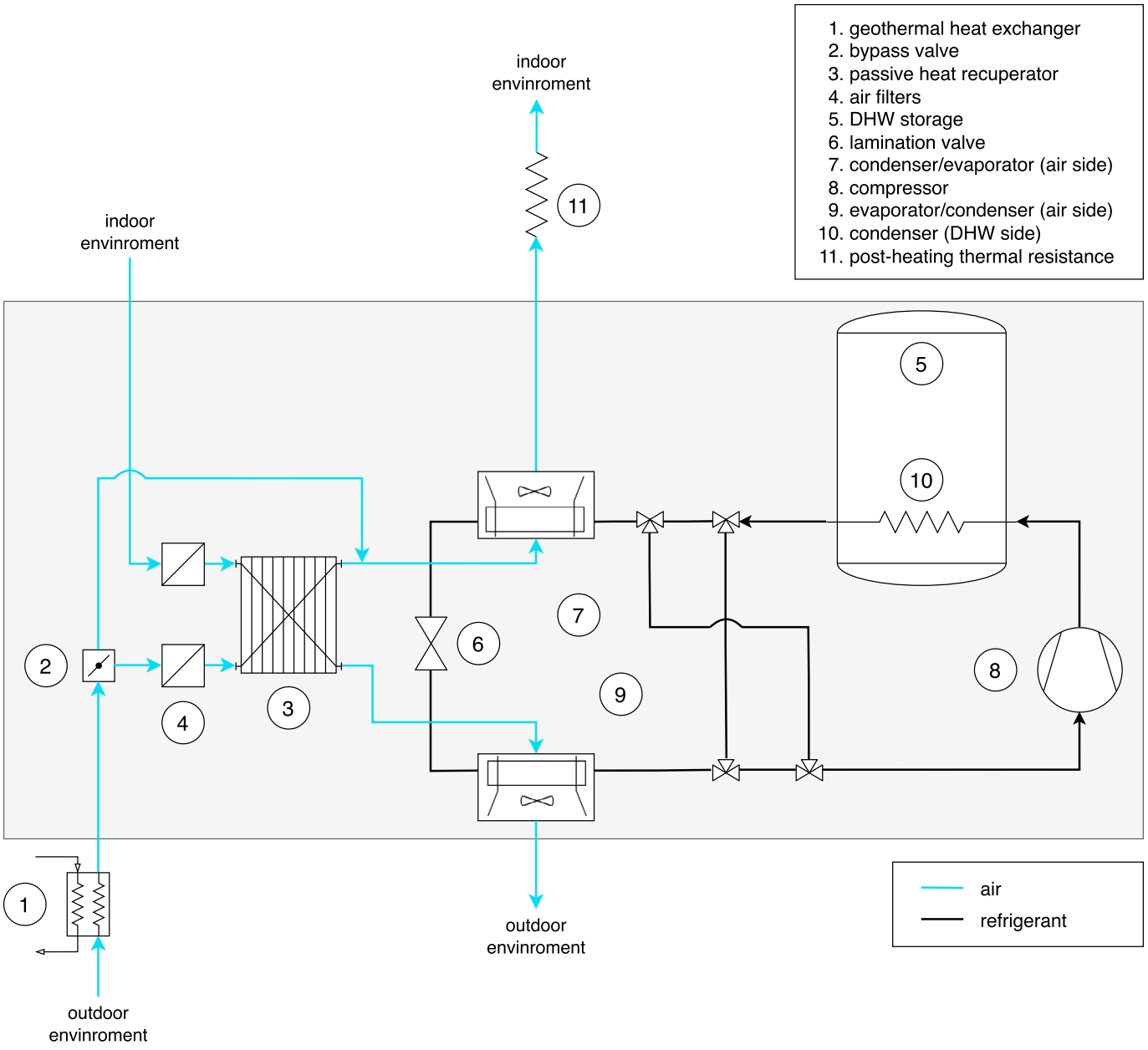

Fig. 1. Simplified layout of the air conditioning unit: air-geothermal heat exchanger (component 1); heat pump unit (components 2-10), and integrative post-heating thermal resistance (11).

Table 1
Heating and cooling performance sheet of the heat pump unit. t_{IN} and t_{OUT} were the indoor and outdoor air temperature.

Heating										
Q	[m^{3}h^{-1}]		100			180			220	
t_{IN}	[°C]		21			21			21	
t_{OUT}	[°C]	7	2	-7	7	2	-7	7	2	-7
COP	[-]	2.23	2.16	2.04	3.1	2.77	2.15	3.62	3.21	2.2
$P_{Th,TOT}$	[kW]	1.02	1.11	1.23	1.56	1.68	1.95	1.88	2.10	2.28
P_{Comp}	[kW]	0.30	0.28	0.25	0.30	0.28	0.24	0.29	0.28	0.25
Cooling										
Q	[m^{3}h^{-1}]		180			220			320	
ϕ	[%]		60			60			60	
t_{IN}	[°C]		24			24			24	
t_{OUT}	[°C]	40	35	30	40	35	30	40	35	30
EER	[-]	2.26	2.50	2.66	2.60	2.83	3.37	2.74	2.98	3.47
$P_{Th,TOT}$	[kW]	1.85	1.64	1.34	2.19	1.86	1.52	2.74	2.24	1.68
P_{Comp}	[kW]	0.42	0.40	0.38	0.42	0.40	0.38	0.42	0.40	0.38

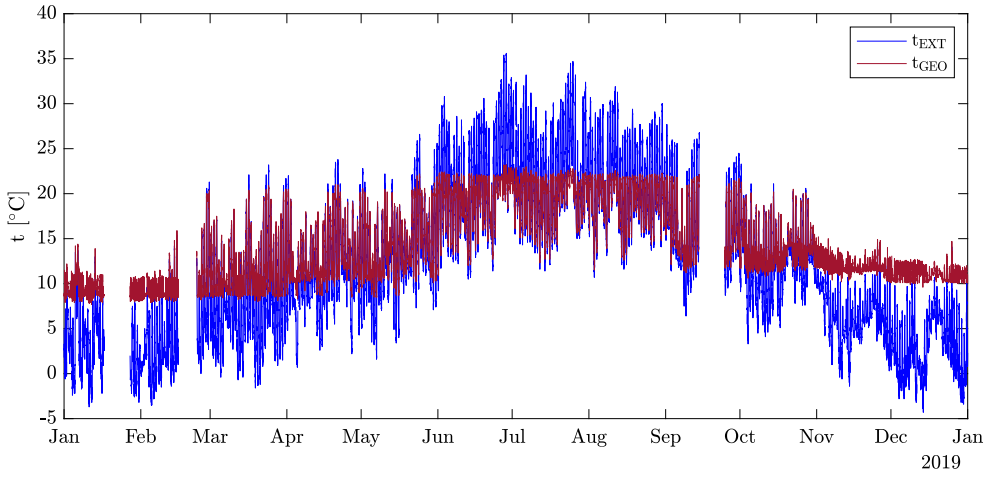

Fig. 2. Evolution of the external temperature (t_{EXT}) (at the inlet of the air-geothermal heat exchanger - blue curve) and the pretreated temperature (t_{GEO}) (at the outlet of the air-geothermal heat exchanger - red curve) in 2019. (For interpretation of the colours in the figure(s), the reader is referred to the web version of this article.)

was in counterflow configuration and made of polystyrene with a declared efficiency of 95%.
- The heat pump equipped with the air-side condenser/evaporator (components 7 and 9), the DHW side condenser (component 10) and the hermetic compressor (component 8).
- The DHW tank (component 5) with a capacity of 180 litres.
- Centrifugal fans to supply the conditioned air and extract the exhaust air, operating at three different rotation rates.

The manufacturer [23] described various operating modes in which the heat pump can work or not depending on the temperature of the inlet air, the indoor temperature requirements, and the demand for DHW. The change in the different operating modes is achieved by activating the bypass valves (for example, component 2 in Fig. 1) and changing the role (from condenser to evaporator and vice versa) between air-side heat exchangers (components 7 and 9 in Fig. 1).

In heating mode, the exhaust air from the indoor environment flowed into the passive heat exchanger (component 3), where it was heated or cooled, depending on the season, by the outdoor air. If this passive heat recovery was sufficient to guarantee indoor comfort, the heat pump did not start to operate for heating purposes, and the power consumption was due only to the ventilation components (that is, the passive heating operating mode shown in Fig. 1). Otherwise, when passive heat recovery was not enough to guarantee internal comfort (or when DHW production is primary required), the heat pump was put into operation (that is, active heating operating mode). In this case, additional heat is extracted from the exhaust air to have evaporation of the refrigerant fluid (component 7 in Fig. 1). Then, after compression, the refrigerant released heat to the DHW tank and to the air supply in the condenser (component 9 in Fig. 1).

During the mid-season, when the air supplied to the heat pump unit (that is, outdoor air in the case of direct supply or air pretreated by the air-geothermal heat exchanger as in this case study) already had adequate conditions to satisfy the indoor comfort requirements, the bypass valve (component 2) is activated, and the inlet air directly supplies the internal environment, without any heat exchange (total by pass operating mode). Even in this operating mode, the heat pump was not activated and the power consumption was due only to ventilation.

In the summer season, if the temperature of the air supplied to the heat pump unit was too high to meet the cooling needs, the compressor started to operate and the air was further cooled in the evaporator (component 6) before discharged indoors (that is, active cooling).

Regarding the heat pump refrigerant, after it evaporated in the evaporator, it reached the compressor and transferred heat to the exhaust air in the condenser (component 9) and in the DHW tank.

2.1. Integrative post-heating thermal resistance

The analysed heating system was rounded off by an integrative post-heating resistance, which entered into operation when the heat pump unit did not reach the temperature required by the environment or in the case of high demand for DHW. The maximum power absorbed by the thermal resistance was equal to 1 kW.

2.2. On-board monitoring system

The system was equipped with an on-board monitoring system that allowed us to measure only some operating parameters. In particular, the monitoring system acquired every 60 seconds the outdoor and indoor air temperatures, the air temperature at the outlet of the air-geothermal heat exchanger, the supply air temperature and the relative humidity of the outdoor air. An example of data provided by the monitoring system is reported in Fig. 3. The power consumption of the heat pump unit and the integrative post-heating resistance, the rotation rate as a percentage of the fans, and the relative humidity in the home were also measured, but at a lower frequency: every five minutes.

3. Heat pump model and data analysis

To identify and separate the different factors that affect the performance of the heat pump under real operating conditions, it was necessary not only to simulate the performance of the system under the monitored operating conditions but also to predict the variation of this performance in the case of different operating regimes, such as those occurring without the air-geothermal heat exchanger. However, it was well known (but also clear in Table 1) that the performance of a heat pump depended on several parameters, which generally vary in real operating conditions, such as, for example, the temperature of the outdoor and indoor air.

Since the on-board monitoring system did not provide all the data needed to develop and calibrate the heat pump model (such as, for example, the flow rate), it was first necessary to analyse the available data and determine the missing information. Then, to carry out this analysis, it was necessary to develop a numerical model capable of reproducing the performance of the system under real operating conditions with variable parameters.

Before entering into the details of the analysis, it is important to note that the available data were processed in the MATLAB environment [24] by adopting the CoolProp database [25] for the calculation of air properties.

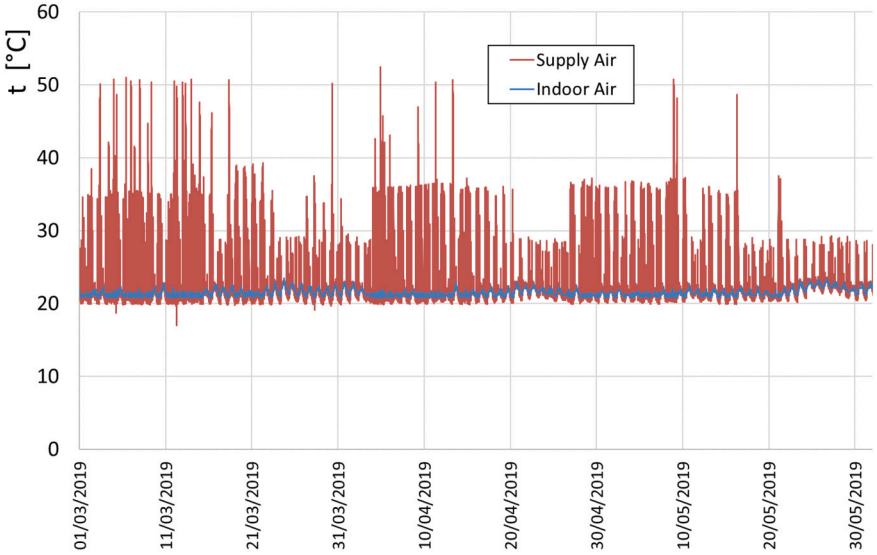

Fig. 3. Example of data provided by the monitoring system: evolution of the supply and indoor temperatures during the period from March to May 2019.

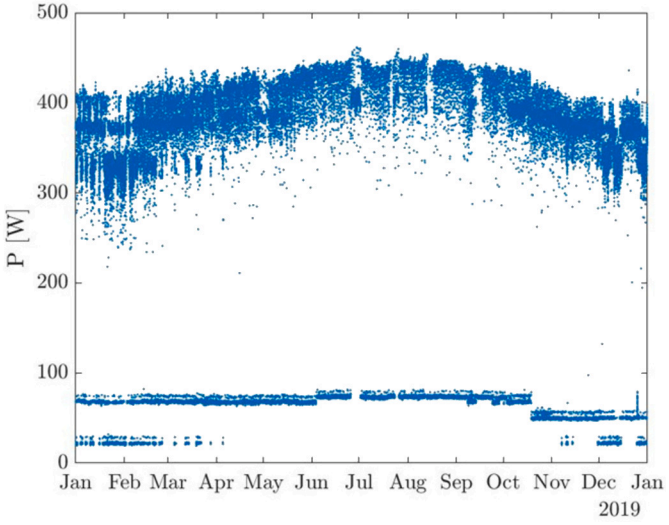

Fig. 4. Heat Pump electrical power consumption in 2019.

3.1. Model of the ventilation system

Generally, the performance of the heat pump was directly related to the electric consumption of its compressor. However, the monitoring system of this unit - as in general that of all commercial domestic units - only provided total electric consumption, including compressor consumption and forced mechanical ventilation (Fig. 4). Therefore, to separate the two contributions, it was necessary to develop a model capable of estimating the ventilation consumption and then, by subtraction from the total, to determine the compressor quota.

It is clear from Fig. 4 that the lower values of power consumption were related to the operating modes in which the heat pump was not activated (such as passive heating and total bypass operation) and therefore can be attributed to ventilation. Having stated this, it was possible to determine that the minimum demand for ventilation was approximately 12 W during the winter season, while during the summer this consumption increased up to 60 W. However, mechanical ventilation regulated the flow rate by varying the speed of rotation of the fan. In particular, the unit had three possible operating regimes that the control system set based on several parameters, such as outdoor and indoor temperatures and humidity.

To model this regulation strategy, the similarity laws can be applied and, in particular, the ones correlating two different fan operating points in terms of the flow rate Q_v $[m^3\ s^{-1}]$, rotation speed n $[rpm]$ and energy exchange ΔE $[J\ kg^{-1}]$, according to the following equations:

$$Q_{v_2} = Q_{v_1} \cdot \frac{n_2}{n_1} \qquad \Delta E_2 = \Delta E_1 \cdot \left(\frac{n_2}{n_1}\right)^2 \tag{1}$$

The energy exchange, ΔE, of the fans is generally approximated by the increase in pressure Δp:

$$\Delta E \approx \left(\frac{\Delta p}{\rho}\right) \tag{2}$$

resulting in a power consumption equal to:

$$P_{fan} = \frac{\Delta p \cdot Q_v}{\eta(Q_v)} \tag{3}$$

where $\eta(Q_v)$ is the efficiency of the fan, modelled as a quadratic function of the volumetric flow rate.

It must be pointed out that these equations refer to non-compressible fluids but are generally used also for compressible ones in the case of compression ratios below 1.1. This is generally the case for fans, which are normally characterised by a low increase in pressure Δp to compensate for pressure losses in the circuit.

Knowing the rotation rates n of the fan and estimating the mean static pressure losses (and hence Δp for the above mentioned reasons) equal to 600 Pa for both the supply and exhaust air circuits, it was possible - through an iterative process - to properly model the behaviour of the fans, determining the flow rates and power consumption in the three operating regimes (Table 2). It should be noted that the lowest operating regime was characterised by two different rotation rates (38 and 35%), depending on the activation or not of the heat pump compressor.

The values of the ventilation power consumption estimated by the developed model are in good agreement with those measured when the compressor was off.

After the ventilation model development and calibration, it was possible to estimate the fan consumption at all operating points and hence subtracting it from the total power consumption, determining the power absorbed by the compressor of the heat pump unit during the entire monitored year.

The modelling of the ventilation system also allowed us to:

- In-depth investigation of the fluctuations in power consumption of the unit over the year. It is clear from Fig. 4 that the electri-

Table 2
Estimated fan performance in the three operating regimes. The subscripts SUP and EX refer to the supply or the exhaust air circuit, respectively.

	$(n/n_{des})_{EX}$ [%]	$(n/n_{des})_{SUP}$ [%]	Q_{EX} [m^3h^{-1}]	Q_{SUP} [m^3h^{-1}]	Δp [Pa]	η_{EX} [%]	η_{SUP} [%]	P_{fans} [W]
3rd Velocity	75	65	276	239	600	79	79	60.5
2nd Velocity	65	55	239	202	600	79	74	40.1
1st Velocity (compressor on)	38	35	140	129	600	53	48	12.9
1st Velocity (compressor off)	35	25	129	92	600	48	26	12.6

cal power absorbed did not exceed 450 W in the summer season and fluctuated around 380 W in the winter period. These annual fluctuations in peak power are strictly related to ventilation power requirements because of the variation of the rotation speed imposed by the control strategy, which is discussed in the following.

- Determine the air flow rate that flowed through the heat pump at each operating point, whose value was not monitored by the on-board monitoring system.

3.2. Model of the passive heat recuperator

The second phase of the modelling activity requires the definition of the heat exchanges in the heat pump unit. In particular, knowing the air flow rates (see Section 3.1), it was necessary to develop a model that allowed us to estimate the efficiency ε of the passive recuperator (component 3 in Fig. 1).

$$\varepsilon = \frac{(t_{PASS} - t^*)}{(t_{EX} - t^*)} \qquad t^* = \{t_{GEO}, t_{OUT}\} \tag{4}$$

where t_{PASS} and t_{EX} are the temperatures of the air supplied at the outlet of the passive recuperator and of the exhaust air, respectively. t^* is the temperature of fresh air at the inlet of the passive recuperator, which is equal to the temperature at the inlet of the air-geothermal heat exchanger (t_{GEO}) (in this case study) or to the outdoor temperature (t_{OUT}) in the absence of the air-geothermal heat exchanger.

Since t_{PASS} was unknown, to properly calibrate the passive recuperator efficiency model, the operating modes in which the heat pump was not activated (passive heating and total bypass modes) were considered. In particular, for the total bypass mode, excluding the contributions of the passive heat recuperator and heat pump, the temperature variation $\Delta t = t_{SUP} - t^*$ of the fresh air was only due to its flow within the system circuit.

Analysis of temperature data in this mode allowed us to estimate an average increase in the temperature of fresh air $\Delta t = +2\,°C$ in summer and an average decrease $\Delta t = -1\,°C$ in winter. Therefore, focusing on the operating points characterised only by passive heating (in winter), it was possible to determine the efficiency of the recuperator by modifying Equation (4) as follows:

$$\varepsilon = \frac{(t_{SUP} - \Delta t - t^*)}{(t_{EX} - t^*)} = \frac{(t_{SUP} + 1° - t^*)}{(t_{EX} - t^*)} \qquad t^* = \{t_{GEO}, t_{OUT}\} \tag{5}$$

where t_{SUP} is the temperature of the indoor air supplied.

The resulting efficiency values were properly fitted with second-order degree polynomial functions depending on the operating regime/flow rate and on t^* (see Fig. 5).

The efficiency correlations $\varepsilon = f(t^*, Q_{SUP})$, shown in Fig. 5, were used to model the behaviour of the passive recuperator in the winter season and, in particular, to determine the temperature of the fresh air in the outlet section of the passive recuperator, t_{PASS}, at all operating points, including those with the heat pump activated, with or without the geothermal heat exchanger:

$$t_{PASS} = \varepsilon \cdot (t_{EX} - t^*) + t^* \qquad t^* = \{t_{GEO}, t_{OUT}\} \tag{6}$$

Then, to derive the thermal power exchanged in the recuperator, a mean air density was determined on the basis of the mean temperature.

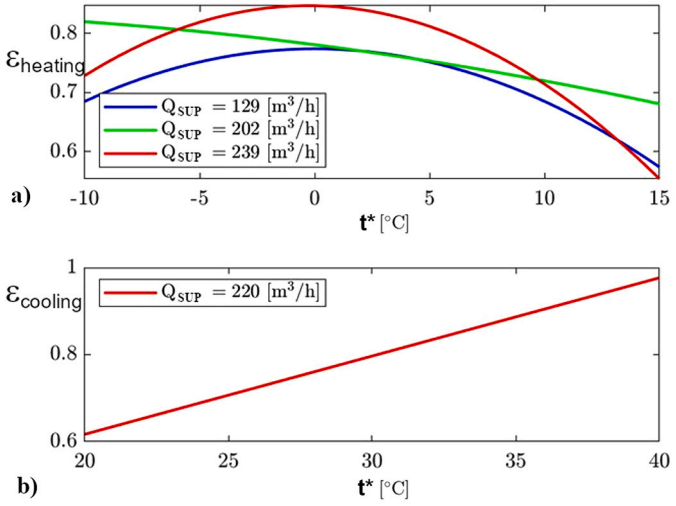

Fig. 5. Efficiency of the heat passive recuperator as a function of the temperature of the air at its inlet t^* and on the operating regime in (a) heating and (b) cooling mode.

$$\overline{\rho_{PASS}} = f\left(\frac{t_{PASS} + t^*}{2}, p\right) \tag{7}$$

where p is the ambient pressure and $f(\cdot)$ is the CoolProp call using those input values.

Therefore, the thermal power exchanged in the passive heat exchanger was computed as

$$P_{th,PASS} = \overline{\rho_{PASS}} \cdot Q_{SUP} \cdot (h_{PASS} - h^*) \tag{8}$$

where h_{PASS} and h^* are the air enthalpy at the temperature t_{PASS} and t^*, respectively.

The modelling of the recuperator behaviour during the cooling season was more complex to develop due to the possible occurrence of a dehumidification process. The temperature of the exhaust air leaving the passive heat exchanger ($t_{PASS}|_{EX}$) was first calculated as follows:

$$t_{PASS}|_{EX} = \varepsilon \cdot (t^* - t_{EX}) + t_{EX} \qquad t^* = \{t_{GEO}, t_{OUT}\} \tag{9}$$

leading to the following thermal power exchange:

$$P_{th,PASS} = \overline{\rho_{PASS}} \cdot Q_{EX} \cdot (h_{PASS}|_{EX} - h_{EX}) \tag{10}$$

where $h_{PASS}|_{EX}$ and h_{EX} are the enthalpy values of the exhaust air at the outlet and inlet of the passive recuperator, respectively.

Knowing the thermal power exchange in the recuperator, it was possible to determine the enthalpy of the outlet supplied air, h_{PASS}:

$$h_{PASS} = h^* - \frac{P_{th,PASS}}{\overline{\rho^*_{PASS}} \cdot Q_{SUP}} \tag{11}$$

where $\overline{\rho^*_{PASS}}$ is evaluated from the values t_{EX} and t^* since t_{PASS} was not already known.

Finally, the temperature of the air supply at the outlet of the recuperator, t_{PASS}, was determined assuming the absolute humidity according

Table 3
Average values of COP and EER of the heat pump unit integrated with the air-geothermal heat exchanger.

Heating										
Q	[m^{3}h^{-1}]		129			202			239	
t_{IN}	[°C]		21.5			21.5			21.5	
t_{OUT}	[°C]	9	/	/	9	/	/	9	/	/
COP		2.52	/	/	3.56	/	/	3.79	/	/
Cooling										
Q	[m^{3}h^{-1}]		/			239			/	
ϕ	[%]		/			variable			/	
t_{IN}	[°C]		/			24			/	
t_{OUT}	[°C]	/	/	/	/	/	24	/	/	/
EER		/	/	/	/	/	2.70	/	/	/

to the dew point and t^*. If the estimate $t_{PASS}|_{EX}$ from Equation (9) was lower than the dew point, a relative humidity φ equal to 99% was assumed (unitary bypass factor hypothesis), allowing us to estimate actual t_{PASS} through the CoolProp database.

$$t_{PASS} = f\left(h_{PASS}, p, \varphi\right) \tag{12}$$

4. Results

As mentioned previously, the purpose of the study is to investigate the behaviour of an air-geothermal heat pump system to identify the main factors that affect the performance of the system under real operating conditions and to quantitatively determine the reduction in energy consumption due to the integration of the air-geothermal heat exchanger in the heating/cooling system.

To this end, in the first part of the analysis, the model was used to investigate the performance of the heat pump system in the installed configuration to identify the main causes of possible differences with the performance under the design conditions declared by the manufacturer in the product specifications (Section 4.1). Then, in the second part, the model was used to simulate the performance of the system in a configuration without the air-geothermal heat exchanger to quantify the reduction in energy consumption due to its air pretreatment (Section 4.2).

4.1. Heat pump performance with the geothermal heat exchanger

Once the ventilation system and passive heat recuperator behaviour were modelled (Section 3.1 and 3.2), it was easy to determine all thermal power exchanges of the heat pump unit on the air side and hence the efficiency values (COP and EER - Energy Efficiency Ratio) according to the following equation.

$$COP, EER = \frac{P_{th,AIR}}{P_{HP} - P_{fans} - P_{reg}} \tag{13}$$

where P_{HP} is the unit consumed power, $P_{th,AIR}$ is the thermal power that the Compact P unit released to the supply air by the active heat recovery operating mode and P_{reg} is a constant power consumption due to the standby and control processes set equal to 9 W according to the technical specifications provided by the system manufacturer.

Table 3 lists the average COP and EER values determined by the mathematical model of the system under real operating conditions for the year 2019. To favour the comparison with the performance declared by the manufacturer on the product sheet (Table 1), the table is organised with the same structure as the product sheet, but only the spots with similar boundary conditions were filled.

In particular, it must be pointed out that

- The flow rates in real operating conditions were slightly different from the ones considered in the data sheet (see Table 1). This is due to the ventilation control system, which regulates the fan rotation rates. In particular, for the cooling mode, the comparison in terms of EER is limited to the operating flow rate equal to 239 m^{3}h^{-1}, which is close to the second one in the manufacturer data sheet 220 m^{3}h^{-1}.
- The exhaust air from the indoor environment, t_{IN}, assumed a temperature of almost 21.5 °C in winter and 24 °C in summer, very close to those of the data sheet: 21 °C and 24 °C.
- The air temperature at the heat pump inlet was not the outdoor temperature t_{OUT}, as in the manufacturer's data sheet, but it was the air temperature at the outlet of the geothermal heat exchanger, t_{GEO}.
- For the heating mode, since the geothermal heat exchanger guarantees at the heat pump inlet an almost constant temperature t_{GEO} of about 9-10 °C, the comparison must be made with the case of an external air temperature t_{OUT} of 7 °C as given in Table 1.
- For the cooling mode, the lowest outdoor temperature in the manufacturer's data sheet is 30 °C, which was never reached in the present case due to the air-geothermal pre-cooling (24 °C).
- The product sheet refers to an external air humidity condition (e.g. 60%) that never occurred in the case study.

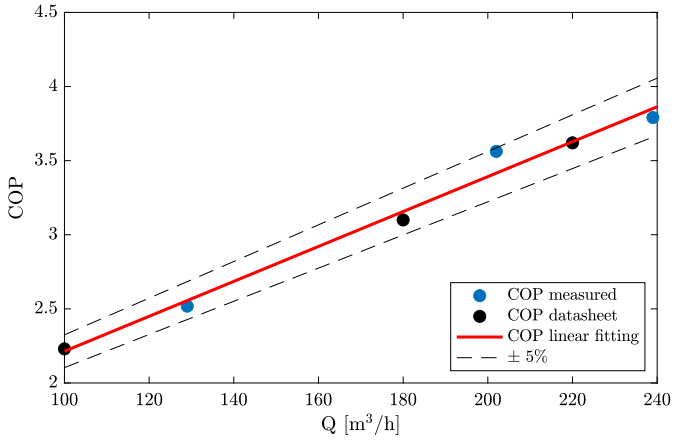

Fig. 6. COP as a function of the operating flow rate: comparison between the measured values in real operating conditions (blue dots) and manufacturer's data listed in the datasheet (black dots).

For the heating mode, due to the differences in flow rates between the real case study and the manufacturer's data sheet, the COP values were given as a function of the flow rate (Fig. 6).

The agreement between the data is very good with a maximum deviation of 5%, which can be considered acceptable due to the assumptions in the model and the different temperature values of the air at the inlet of the heat pump unit (7 vs. 9-10 °C).

In the summer period, as highlighted above, the differences in terms of outdoor temperature and humidity prevent a direct comparison of

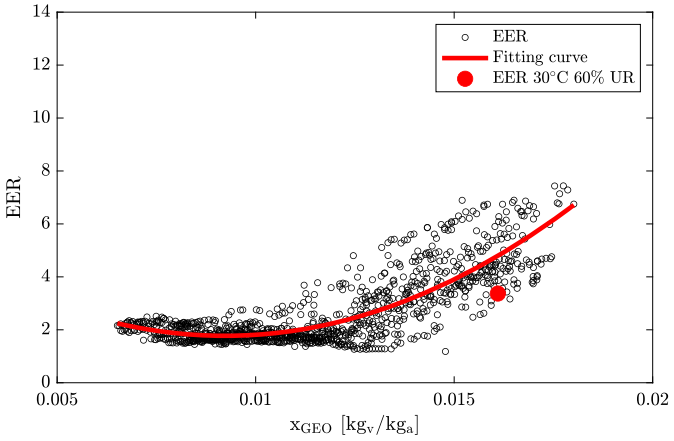

Fig. 7. EER as a function of the air specific humidity at the outlet of the air-geothermal heat exchanger. The EER in the product data sheet (red dot) refers to a relative humidity of 60% and an external temperature of 30 °C.

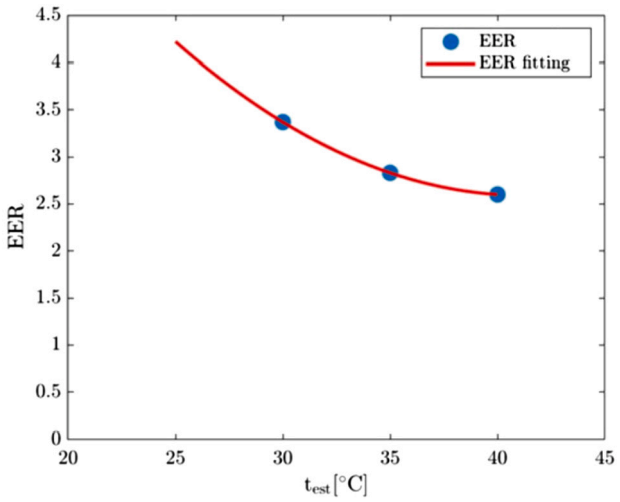

Fig. 8. Regression of the EER values on the product data sheet as a function of the external temperature.

the average EER value listed in Table 3 with the one provided by the manufacturer (Table 1). For example, in the case of different humidity values and the dehumidification process, the EER changes as a result of the removed latent heat.

To make a fair comparison between design and real performance, the EER values were plotted as a function of the air humidity estimated at the outlet of the air-geothermal heat exchanger (Fig. 7).

The EER value reported on the product data sheet (red dot in Fig. 7) is within the band of the experimental values but in the lower range. The main reason is related to the external temperature of 30 °C, which is significantly higher than in the case study (24-25 °C). Note that the EER in the data sheet refers to a relative humidity of 60% and an external temperature of 30 °C.

To confirm this hypothesis, the EER values reported in the product sheet were interpolated as a function of external temperature (Fig. 8). The regression clearly shows that for a temperature of 24 °C, the expected EER is higher than 4, which is in line with the experimental data at the relative humidity of 60% (Fig. 7).

Fig. 7 also shows a clear dependence of the EER on humidity values and a dispersion band amplified at high humidity values. The scattering of the EER values may be linked to the uncertainties of the model in the estimation of the humidity, and hence of the latent heat. To confirm this hypothesis, the EER values were recalculated, excluding the contribution of the latent heat of the dehumidification process (Fig. 9).

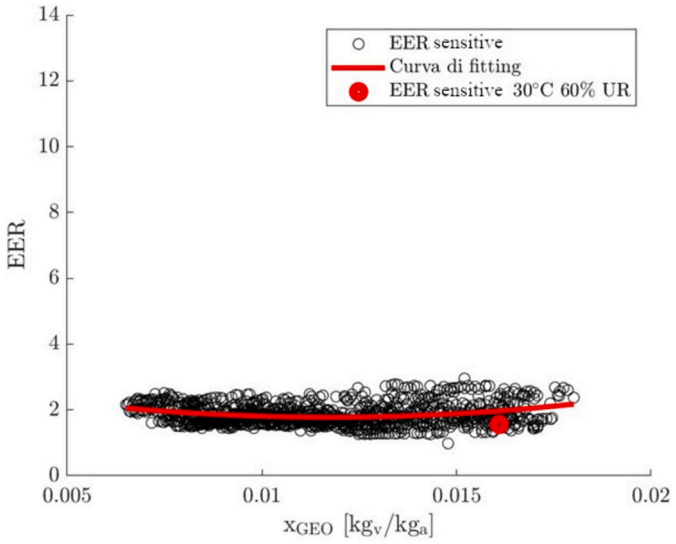

Fig. 9. Average values of the sensitive EER (evaluated without the contribution of latent heat) as a function of the air specific humidity at the outlet of the air-geothermal heat exchanger. The EER on the manufacturer's data sheet (red dot), which refers to a relative humidity of 60% and an external temperature of 30 °C, is also reported without the contribution of latent heat.

The results show a significant reduction in the scatter band and also an increased agreement of the EER values between the manufacturer data and the case study.

4.2. Contribution of the air-geothermal heat exchanger on the reduction of the heat pump consumption

After validation, the mathematical model was used to analyse the influence of the air-geothermal heat exchanger on the efficiency of the heat pump. As discussed in Section 4.1, the performance of the system varies (even significantly in some cases) depending on several factors; certainly, one of them is the inlet temperature. To properly quantify the benefits derived from the integration of the air-geothermal heat exchanger with the unit energy consumption, it was necessary to investigate the performance of the system in a configuration without the air pretreatment provided by the air-geothermal heat exchanger.

As explained above, the MATLAB heat pump model was developed to allow analysis with and without the air-geothermal heat exchanger, considering the outdoor temperature t_{OUT} as the value of the air temperature at the inlet of the passive heat recuperator.

With respect to the model settings, the following hypotheses were applied.

- The air supplied to the internal environment was considered equal in both cases to guarantee the same level of comfort.
- Due to the lack of a contribution of the air-geothermal heat exchanger, the post-heating resistance of the heat pump system was expected to play a more important role. In particular, for values of compressor power less than 200 W, the heat pump unit was deactivated and the heat demand was satisfied only by the post-heating resistance.
- The operating regime of the ventilation system was assumed to be the same in terms of fan rotation speed and flow rates in both cases.
- In both cases, the power consumption of the ventilation system was assumed to be equal. The same was done for the power consumption of the DWH production.

Fig. 10 shows the comparison of the daily energy exchanged by the components of the system between the two configurations with (a) and without (b) the air-geothermal heat exchanger. Positive values refer to

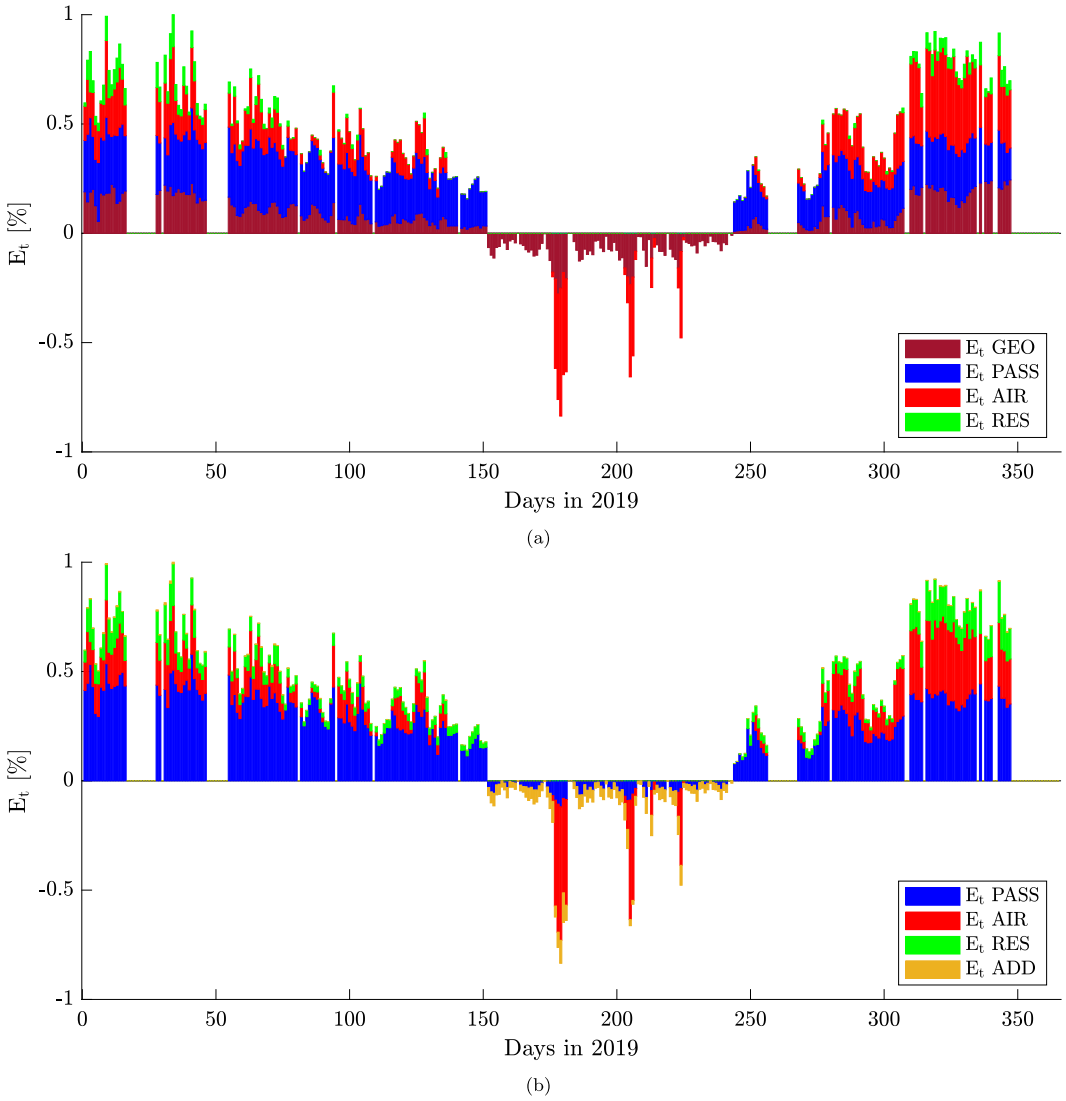

Fig. 10. Comparison of daily energy exchanged per system component (in percentage of the maximum daily energy exchange) between the configurations with (a) and without (b) the air-geothermal heat exchanger. Positive values refer to the thermal energy in the winter season, whereas negative values refer to the cooling needs in summer period.

the thermal energy in the winter season, whereas negative values refer to the cooling energy in the summer. Since the installed heating system may not meet the required heat load without the geothermal contribution, an additional heat input was included in the configuration and was used by the algorithm to reach the required indoor air temperature.

Due to the climatic zone of the location of the analysed building (zone F), the system is characterised by a higher thermal demand in the winter season than in the summer one.

To cover winter demand, the air-geothermal heat exchanger and the passive recuperator play a key role, producing almost 50% of the maximum thermal energy demand in the original configuration (Fig. 10a). The absence of the contribution of the air-geothermal heat exchanger leads to a larger use of the passive recuperator and, to a lower extent, of the integrative post-heating resistance (Fig. 10b). It is also fundamental to note that no contributions from the additional heat source were required.

During the summer season, the passive recuperator was unable to fully compensate for the missing cooling contribution of the air-geothermal heat exchanger, and the demand was satisfied by increasing the contributions of the heat pump and of the additional source to reach the same indoor conditions (Fig. 10b).

The different contributions in terms of thermal exchange are also reflected in the electrical consumption of the heat pump system. Fig. 11 shows the daily electrical consumption by component, also considering the production of DHW.

As shown in Fig. 10, in the winter season, the passive heat exchanger was only partially capable of covering the missing contribution of the air-geothermal heat exchanger, forcing an increase in the use of the post-heating resistance, whose electric consumption increases (Fig. 11).

In summer, the electrical consumption was only apparently similar. In fact, it should be noted that an additional cooling source was required to meet the cooling needs of the building, and this was not considered in Fig. 11.

To provide a more accurate indication of energy consumption, Table 4 lists the overall values and the percentage of the total, regarding the present scenario (with air-geothermal heat exchanger), for each component.

The consumption of electricity in the winter season increased by approximately 30% without the contribution of the air-geothermal heat exchanger, with a clear increase in the activation of the post-heating resistance. The higher consumption of thermal resistance and the additional power required have shown that the Compact P unit operated in

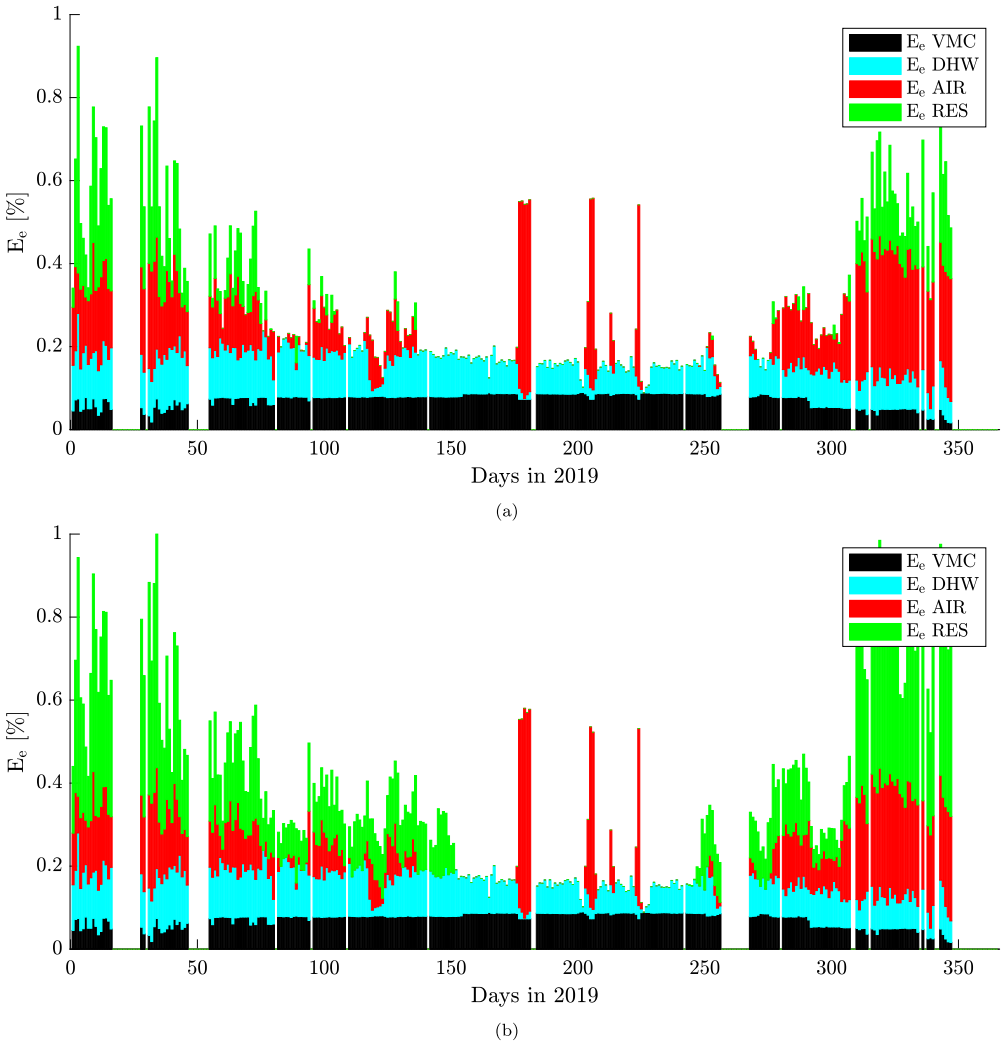

Fig. 11. Daily electricity consumption in 2019 with (a) and without (b) the air-geothermal heat exchanger. Histogram data plots refer to cumulative energy per day as a percentage of maximum electricity consumption in the same year.

Table 4
Total thermal and electrical energy showing percentage contribution of each component referred to the installation of the air-geothermal heat exchanger.

		Heating		Cooling	
		GEO	NO GEO	GEO	NO GEO
E_{th}	[kWh]	5400.9	5400.9	-579.2	-579.2
GEO	[%]	21.2	-	64.2	-
PASS	[%]	46.4	61.8	-	24.8
AIR	[%]	27.7	24.6	35.8	39.7
RES	[%]	4.7	13.0	-	-
ADD	[%]	-	0.7	-	35.5
E_{el}	[kWh]	1297.0	1693.5	306.5	306.8
VMC	[%] on GEO	19.0	19.0	43.0	43.0
DHW	[%] on GEO	27.8	27.8	32.4	32.4
AIR	[%] on GEO	33.5	29.8	24.6	24.7
RES	[%] on GEO	19.8	54.0	-	-

a regime of nearly maximum capacity. So, if necessary, the compressor power could not increase too much due to operating limits.

5. Conclusions

The study presents an in-depth analysis of the performance of a heat pump under real operating conditions to highlight the parameters that affect the performance compared to the manufacturer's design characteristics. The case study was an independent single-family building located in north Italy and equipped with an HVAC system consisting of an air-geothermal heat exchanger coupled with a compact unit supported by an electrical heater to meet peak demands. The system was properly modelled in the Matlab environment to evaluate the system performance under different operating conditions (real and simulated). The data acquired by the onboard monitoring system during one year of operation of the heat pump were used to properly develop, calibrate, and validate the model. The model was then used for two different purposes. First, we analysed the unit performance under real operating conditions and the existence of factors more or less significantly affecting the performance. Second, we quantitatively analyse the benefits deriving from the combination of the system with an air-geothermal heat exchanger.

Regarding unit performance under real operating conditions, the comparison highlighted that, for the same air inlet conditions (temperature and humidity) and system operating conditions (ventilation flow rate), unit performance in both heating and cooling modes agreed well with the data provided by the manufacturer. However, the analysis also confirmed the influence of several factors on performance, as well as the relevance of considering these factors in feasibility studies and/or in the definition of optimal control strategies. In particular, in the heating mode, one of the factors affecting unit performance was ventilation air, defined by the control strategy: the analysis showed that the minimisation of indoor ventilation in the event of low outdoor temperatures

was of paramount relevance not only because it reduced the indoor heat demand, but also because it maintained the unit efficiency closer to the design conditions. Note that the minimum ventilation necessary to maintain the air exchange required by sanitary standards is guaranteed in all conditions analysed. The cooling mode also highlighted the dependence of efficiency on dehumidification. The available technical data refer to a very specific relative humidity condition (60%), which may be far from the real one. This factor can greatly affect the performance of the unit and must be considered.

Regarding the inclusion of the air-geothermal heat exchanger, the analysis confirmed its fundamental role in maintaining unit performance close to that of the design, limiting the influence of variable outdoor air conditions. Thanks to the air-geothermal heat exchanger, the heating and cooling demand was strongly reduced during the year of operation, and even the efficiency of the unit was on average higher because of the almost constant air conditions at the unit inlet guaranteed by the air-geothermal heat exchanger. From a quantitative point of view, the analysis estimated that in winter 2019 without the air geothermal unit, the electricity consumption would be 130% of the measured one, due to the higher thermal demand, which in turn led to a higher operation of the post-heating electrical heater. In summer 2019, the heat pump was unable to meet the house's cooling needs. So, the analysis confirmed the significant benefits deriving from the installation of the air-geothermal heat exchanger, allowing not only to maximise the unit performance but also to limit the unit size, with consequent economic and environmental benefits.

Abbreviations

The following abbreviations are used in this manuscript:

ADD	Additional thermal energy
AIR	Supply air heat pump contribution
CO_2	carbon dioxide
COP	Coefficient of Performance
DHW	Domestic hot water
EER	Energy Efficiency Ratio
EXT	External air conditions
GEO	Geothermal heat exchanger
HVAC	Heating, ventilation, and air conditioning
PASS	Passive heat exchanger (recuperator)
RES	Electrical post-heating resistance
VMC	Mechanical ventilation

Nomenclature

η [-] fan efficiency
$\overline{\rho_{PASS}}$ $[kg\,m^{-3}]$ mean air density in the passive recuperator
ρ $[kg\,m^{-3}]$ air density
ε [-] efficiency of the passive recuperator
φ [-] relative humidity
E $[J\,kg^{-1}]$ air energy per unit of mass
E_{el} $[kWh]$ electrical energy
E_e [%] percentage of the daily electrical energy over the daily maximum electrical energy
E_{th} $[kWh]$ thermal energy
E_t [%] percentage of the daily thermal energy over the maximum daily thermal energy provided by the unit
h^* $[J/kg]$ air enthalpy at the temperature t^*
h_{EX} $[J/kg]$ enthalpy of the exhaust air at the inlet of the passive recuperator
h_{PASS} $[J/kg]$ air enthalpy at the temperature t_{PASS}
n [rpm] fan rotation rate
p [Pa] air pressure
P [W] heat pump power input
P_{Comp} [W] Compressor power
P_{fan} $[W]$ fan power
P_{HP} $[W]$ heat pump input power
P_{reg} $[W]$ power consumption due to the standby and control processes
$P_{th,AIR}$ $[W]$ thermal unit power released to the supply air by the active heat recovery operating mode
$P_{th,TOT}$ [W] Total thermal power
Q $[m^3h^{-1}]$ flow rate
Q_{EX} $[m^3h^{-1}]$ flow rate of the exhaust air circuit
Q_{SUP} $[m^3h^{-1}]$ flow rate of the supply air circuit
t_{GEO} [°C] temperature at the outlet of the air-geothermal heat exchanger
t^* [°C] temperature of fresh air at the entrance of the passive recuperator
t_{EX} [°C] temperature of the exhaust air
t_{IN} [°C] indoor temperature
t_{OUT} [°C] outdoor temperature
t_{PASS} [°C] temperature of the air supplied at the outlet of the passive recuperator
t_{SUP} [°C] temperature of the indoor air supplied
x_{GEO} $[kg_v/kg_a]$ air specific humidity

CRediT authorship contribution statement

Giovanna Cavazzini: Writing – review & editing, Methodology, Investigation, Data curation. **Giacomo Zanetti:** Writing – review & editing, Methodology, Investigation, Conceptualization. **Alberto Benato:** Writing – original draft, Methodology, Investigation, Formal analysis, Data curation, Conceptualization.

Declaration of competing interest

The authors declare the following financial interests/personal relationships which may be considered as potential competing interests: Giovanna Cavazzini reports financial support was provided by ENEA National Agency for New Technologies Energy and Economic Sustainable Development (Rds/PTR2021/140).

Data availability

The data that has been used is confidential.

References

[1] European Commission, Department: energy, energy efficiency in buildings, https://energy.ec.europa.eu/topics/energy-efficiency/energy-efficient-buildings/energy-performance-buildings-directive_en. (Accessed April 2024), December 2023.
[2] European Heat Pump Association (EHPA), European market of the heat pump units and statistics, 2021 Accessed April 2022,.
[3] O. Cauret, Heat pumps in multi-family buildings, drivers and barriers, Heat Pump. Technol. Mag. 29 (1) (2021) 15–21.
[4] ISTAT, Censimento edifici residenziali, http://dati-censimentopopolazione.istat.it/, 2011.
[5] O. Ruhnay, L. Hirth, A. Praktiknjo, Time series of heat demand and heat pump efficiency for energy system modelling, Sci. Data 6 (2019) 1–10.
[6] D. Fisher, T. Wolf, J. Wapler, R. Hollinger, H. Madani, Model-based flexibility assessment of a residential heat pump pool, Energy 118 (2019) 853–864.
[7] D. Günther, M. Miara, R. Langnner, S. Helmling, H. Madani, Wp monitor - feldmessung von wärmepumpenanlagen (Wp monitor - field measurements of heat pumps), final Project Report (Fraunhofer ISE, 2014), 2014.
[8] R. Wang, Z. Jin, X. Zhai, W. Luo, T. Eikevik, Investigation of annual energy performance of a vwv air source heat pump system, Int. J. Refrig. 85 (2018) 383–394.
[9] K.X. Le, M.J. Huang, N.N. Shah, C. Wilson, P.M. Artain, R. Byrne, N.J. Hewitt, Techno-economic assessment of cascade air-to-water heat pump retrofitted into residential buildings using experimentally validated simulations, Appl. Energy 250 (2019) 633–652.
[10] C. Underwood, M. Royapoor, B. Sturm, Parametric modelling of domestic air-source heat pumps, Energy Build. 139 (2017) 578–589.
[11] S. Caird, R. Roy, S. Potter, Domestic heat pumps in the UK: user behaviour, satisfaction and performance, Energy Effic. 5 (2012) 283–301.
[12] K. Huchtemann, D. Müller, Evaluation of a field test with retrofit heat pumps, Build. Environ. 53 (2012) 100–106.

[13] P. Carroll, M. Chesser, P. Lyons, Air source heat pumps field studies: a systematic literature review, Renew. Sustain. Energy Rev. 134 (2020) 110275.
[14] Z. Lu, D. Ziviani, Operating cost comparison of state-of-the-art heat pumps in residential buildings across the United States, Energy Build. 277 (2022) 110275.
[15] A.M. Omer, Ground-source heat pumps systems and applications, Renew. Sustain. Energy Rev. 12 (2) (2008) 344–371.
[16] O. Arslan, A.E. Arslan, T.E. Boukelia, Modelling and optimization of domestic thermal energy storage based heat pump system for geothermal district heating, Energy Build. 282 (2023) 112792.
[17] J. Deng, M. Ma, Q. Wei, J. Liu, H. Zhang, M. Li, A specially-designed test platform and method to study the operation performance of medium-depth geothermal heat pump systems (md-ghps) in newly-constructed project, Energy Build. 272 (2022) 112369.
[18] B. Kulcar, D. Goricanec, J. Krope, Economy of exploiting heat from low-temperature geothermal sources using a heat pump, Energy Build. 40 (3) (2008) 323–329.
[19] T.S. Bisoniya, Design of earth–air heat exchanger system, Geotherm. Energy 3 (2015) 1–10.
[20] N. Rosa, N. Soares, J. Costa, P. Santos, H. Gervásio, Assessment of an earth-air heat exchanger (eahe) system for residential buildings in warm-summer Mediterranean climate, Sustain. Energy Technol. Assessm. 38 (2020) 100649.
[21] C.H. Diedrich, G.H.d. Santos, G.C. Carraro, V.V. Dimbarre, T.A. Alves, Numerical and experimental analysis of an earth–air heat exchanger, Atmosphere 14 (7) (2023) 1113.
[22] Xlam Dolomiti, Xlam website, https://www.xlamdolomiti.it/. (Accessed April 2024).
[23] Nilan, Nilan website, https://www.nilan.dk. (Accessed March 2021).
[24] Mathworks, Matlab r2019a, www.mathworks.it/help/matlab/, 2019. (Accessed December 2022).
[25] I.H. Bell, J. Wronski, S. Quoilin, V. Lemort, Pure and pseudo-pure fluid thermophysical property evaluation and the open-source thermophysical property library coolprop, Ind. Eng. Chem. Res. 53 (6) (2014) 2498–2508.